



# Electrochemical Biosensors for Soluble Epidermal Growth Factor Receptor Detection

Jana Shepa<sup>1</sup> · Ivana Šišoláková<sup>1</sup> · Martin Panigaj<sup>2</sup> · Dominika Bilá<sup>2</sup> · Pavol Jarčuška<sup>3</sup> · Renáta Oriňaková<sup>1</sup>

Accepted: 22 April 2022 / Published online: 4 May 2022

© The Author(s), under exclusive licence to Springer Science+Business Media, LLC, part of Springer Nature 2022

## Abstract

Simple detection of oncomarkers is of paramount importance in cancer diagnosis. Screen-printed carbon electrodes (SPCEs) were modified by streptavidin, which served as a suitable platform for aptamer molecule binding. The electrochemical conditions for soluble epidermal growth factor receptor (EGFR) sensing were studied and optimized. Developed sensors display a wide linear range from 10 to 500 ng/ml and a low limit of detection of 1.19 ng/ml. SPCEs modified by streptavidin could be used not only as an amperometric sensor but also as an impedimetric one. Moreover, SPCEs were successfully tested for soluble EGFR detection in blood serum samples. This platform presents a simple solution for the application of aptamers in electrochemical testing without the multistep working electrode modification processes.

**Keywords** Electrochemical detection · Electrochemical sensors · Electrochemistry · Sensors · Screen-printed carbon electrodes

## Introduction

Biomarkers are biologic features that are monitored to consider normal biological and pathological processes, based on the National Institute of Health Biomarkers Definition Working Group description [1]. Currently, several cancer-relevant proteins have been studied as a potential biomarker, such as carcinoembryonic antigen (CEA), epidermal growth factor receptor (EGFR) in glioblastoma, HER2 and MUC1 in breast carcinomas, CD30 and CD4 in lymphoma cells, epithelial cell adhesion molecule (EpCAM), prostate membrane-specific antigen (PMSA),  $\alpha$ -Fetoprotein (AFP) in hepatocellular carcinoma, and Mucin 1 glycoprotein [2]. The EGFR as one of the biomarkers is a cell trans-membrane

glycoprotein located at the cell surface [3]. Its activation and auto-phosphorylation initiate a series of pathways that control processes such as proliferation, adhesion, migration, and apoptosis [4]. Overexpression of EGFR can lead to deregulation of cell processes and results in the initiation of several types of cancer [5]. EGFR is not the only predictor of the efficacy of targeted non-small-cell lung cancer (NSCLC) therapy [6, 7] but also in the case of breast, gastric, prostate, renal, head, neck, colorectal, bladder, pancreatic, esophageal, and ovarian cancers [3]. In addition to overexpression of EGFR in many types of cancer cells, soluble EGFR (sEGFR) or displayed on the surface of exosomes is released into the blood [8–10].

Many techniques used EGFR for detection. Among these, enzyme-linked immunosorbent assay (ELISA) represents the gold standard for the detection of protein concentration. On the other hand, this technique is complicated and time-consuming [11]. Other methods, immunohistochemistry (IHC) on tissues and western blotting (WB) on membranes, need strong personal skills to perform detection [5]. Recently, several methods were developed for soluble EGFR detection such as microfluidic biochip [12], electrochemical immunosensor for soluble EGFR detection [5, 13, 14], detection via Raman spectroscopy [15], and methods based on quartz crystal microbalance [16].

✉ Ivana Šišoláková  
ivana.sisolakova@upjs.sk

<sup>1</sup> Department of Physical Chemistry, Pavol Jozef Šafárik University in Košice, Moyzesova 11, 040 01 Košice, Slovak Republic

<sup>2</sup> Institute of Biology and Ecology, Pavol Jozef Šafárik University in Košice, Moyzesova 11, 040 01 Košice, Slovak Republic

<sup>3</sup> Department of Infectology and Travel Medicine, Pavol Jozef Šafárik University in Košice, Moyzesova 11, 040 01 Košice, Slovak Republic

In recent years, numerous DNA sensors have been developed to detect specific nucleotide sequences and proteins [17]. The electrochemical sensors for EGFR detection display many advantages in comparison with the above-mentioned methods such as high selectivity and sensitivity, compatibility with modern microfabrication, and miniaturization technologies [18]. Carbon materials possess these properties and are widely used in different types of sensors for various biomolecules detection [19–28]. Various types of carbon materials, such as graphene, nanotubes, glassy carbon, graphite, and their combinations with other materials, were used for sensor fabrication [29]. Among them, materials, screen-printed carbon electrodes (SPCEs) attract tremendous attention. One of the reasons is that the screen-printing method provides precise control over the dimensions, high reproducibility, uniformity, and the ability for mass production [22]. Moreover, SPCE combines portability with simple and inexpensive methods and is easy to use. SPCE could be modified by a wide range of materials via various types of methods. In the case of biomarkers detection, several strategies of electrode modifications could be used.

In general, biosensors could be divided into immunosensors, aptasensors, enzymatic biosensors, and genobiosensors [30]. Aptasensors use nucleic acid aptamers that are immobilized on the conducting surface. The most popular aptasensors material is a gold surface that allows easy immobilization of thiolated aptamers [8]. Many modifications are complicated and display complicated fabrication. The main effort is to eliminate the multistep preparation and complicate the fabrication process. Moreover, it is also favorable to eliminate the use of noble metals such as gold because they increase the price of aptasensor [31].

Aptamers are single-stranded DNA or RNA sequences adopting a specific three-dimensional shape that provides highly specific binding to targeted molecules with an affinity comparable to monoclonal antibodies. Aptamers can be in vitro selected using a process termed systematic evolution of ligands by exponential enrichment (SELEX) [32, 33]. Over the last three decades, aptamers have been developed against a variety of targets, from small metabolites to proteins. In addition, aptamers have been linked to novel constructs involving other functional RNAs, chemotherapeutic agents, and nanoparticles [34]. Besides serving as delivery agents for therapeutic cargo, aptamers can stimulate, or block, targeted cellular proteins [35]. Production of aptamers has several advantages over protein ligands such as antibodies including high-throughput selection, time-saving, scalability, and low immunogenicity; furthermore, aptamers do not require a cold chain, etc. Thus, aptamers seem to be a favorable material for targeted therapies and diagnostics.

Herein, we report a highly sensitive aptasensor for soluble EGFR detection by immobilizing an aptamer molecule on the SPCE modified by streptavidin molecule (SPCEs).

SPCEs represent a simple solution for aptasensor development and offer a favorable environment for aptamer immobilization resulting in satisfactory detection parameters. Moreover, the ferro/ferricyanide solution is frequently used for biomolecule detection via aptasensors because of its well-defined electrochemical properties (oxidation and reduction potential, reversibility of electrochemical reaction, etc.). The binding of biological molecules such as aptamer or EGFR on electrode surface represents a change of phase interface, so influences the electrochemical oxidation/reduction of ferro/ferricyanide molecules. Based on the signal change caused by this behavior, it is possible to evaluate the electroanalytical characteristics of the developed sensor.

The novelty of the work is the simplicity of the modification process. The SPCEs represent an uncomplicated solution without the necessity to use noble metal nanoparticles for the biomolecules anchoring or multistep modification process.

## Methods

### Chemicals and Reagents

Phosphate buffered saline (PBS D8662, sterile filtered) was purchased from Biowest. Sodium hydroxide (NaOH, 99%) and hydrochloric acid were obtained from Milan Adamik, Laboratory Chemicals, and Sigma-Aldrich, respectively. Potassium hexacyanoferrate (II) trihydrate ( $K_4[Fe(CN)_6] \cdot 0.3H_2O$ , p.a. 99%) and potassium hexacyanoferrate (III) ( $K_3[Fe(CN)_6]$ , p.a. 99%) were purchased from CentralChem. All DNA oligonucleotides (for PCR of aptamer template and anchoring the aptamer) were purchased from Sigma-Aldrich. Purified aptamer bound to biotinylated anchoring oligonucleotide was diluted in DPBS supplemented with 5 mM  $MgCl_2$ . Recombinant soluble human EGFR was obtained from the Acro biosystem. Deionized water (18.2  $M\Omega \cdot cm$ ) was used for solution preparation.

### Aptamer Preparation

The specificity of aptasensor is mediated by the J18 RNA aptamer specific to the human epidermal growth factor (EGFR) [36, 37]. Synthetic DNA template (Table 1) (Sigma-Aldrich) coding J18 RNA aptamer has been amplified by polymerase chain reaction (PCR) (Bioline) using a set of primers (Table 1). The 3' end of aptamer was extended with a sequence complementary to a binding biotinylated oligonucleotide (Table 1). The amplified template was purified by Gel and PCR Clean-up kit (Macherey–Nagel) and RNA was transcribed in vitro overnight at 37 °C using T7 polymerase. Residual template DNA present in the transcribed RNA pool was degraded using 0.12 U/ $\mu l$  of DNase I (NEB) at 37 °C for

**Table 1** Sequences used for PCR amplification of DNA template for in vitro transcription of J18 RNA aptamers, including the anchoring biotinylated DNA oligonucleotide. All sequences are in 5'→3' orientation

|   |
|---|
| DNA template                                    |
| GGG CGC TCC GAC CTT AGT CTC TGC AAG ATA AAC CGT |
| GCT ATT GAC CAC CCT CAA CAC ACT TAT TTA ATG TAT |
| TGA ACG GAC CTA CGA ACC GTG TAG CAC A           |
| Forward primer                                  |
| GCG ATA ATA CGA CTC ACT ATA GGG CGC TCC GAC CTT |
| AGT C   |
| Reverse primer                                  |
| CAA AGG CCC GGA TAG CCT CTG CTG TGC TAC ACG GTT |
| CGT A   |
| Biotinylated oligonucleotide                    |
| AAA ACA AAG GCC CGG ATA GC                      |

30 min. Subsequently, the RNA was purified in 8% denaturing polyacrylamide gels containing 8 M urea (Invitrogen). RNA was visualized under UV shadowing using fluorocoded thin-layer chromatography (TLC) plates (Ambion) and excised gel slices containing bands with correct length were incubated in Crush and Soak buffer (1×TBE, 300 mM NaCl) for 30 min at −80 °C and then overnight at 4 °C. After that, the supernatant (500 μl) was mixed with 750 μl of 100% ethanol and incubated at −20 °C for 1–3 h. Subsequently, RNA was precipitated by centrifugation at 4 °C, 21 000×g for 30 min. The pellet was washed with 90% ethanol by spinning at 4 °C, 21 000×g for 10 min. Finally, the RNA pellet was dried up on air for 10 min and then resuspended in DNase/RNase free water. The concentration and purity of RNA were determined by NanoDrop (Thermo Fisher Scientific).

To ensure binding of the aptamer to streptavidin-coated probes, the J18 aptamer was base-paired to the single-stranded biotinylated DNA oligonucleotide (B-oligo) (Sigma-Aldrich). A 1:1 molar ratio of the aptamer to the DNA oligonucleotides biotinylated at the 5'-end was used. Hybrid formation involved heating the sample for 3 min at 73 °C with a subsequent gradual decrease to 25 °C.

## Electrochemical Measurements

The streptavidin-modified SPCEs used for all measurements were purchased from Metrohm (Utrecht Netherlands). Three electrode system consisted of the carbon-streptavidin working electrode (4 mm diameter), silver pseudo reference electrode, and carbon counter electrode. Electrodes were rinsed with distilled water and dried on air in a laminar box. 10 μl of aptamer-B-oligo was dropped on the electrode surface and stored in the fridge for 2, 5, 10, 30, and 60 min at 4 °C. Then, electrodes were rinsed with PBS solution and dried on air. Modified electrodes were stored in the fridge at 4 °C. Recombinant soluble

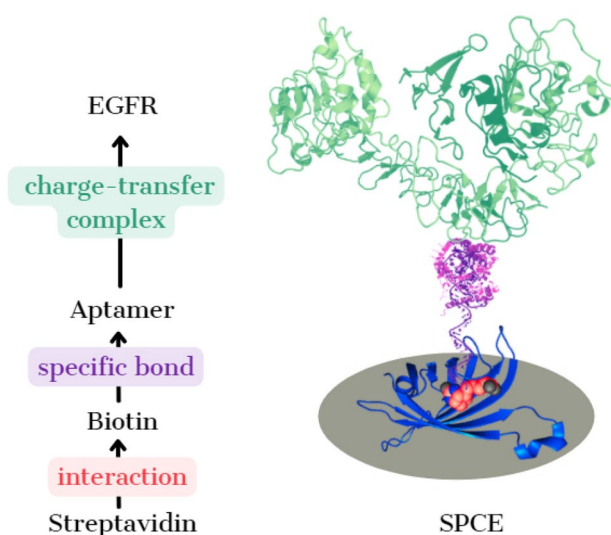


**Fig. 1** Schematic illustration of sensor principle

human EGFR was diluted in the solution of 0.1 M ferro/ferricyanide in PBS. Cyclic voltammetry was used for the study of the electrochemical behavior of prepared electrodes and measurements were performed from the potential −1 V to 1 V at the various scan rates 20, 50, 70, 100, and 200 mV/s to consider the mechanism of electrochemical reaction. To study detection properties, all measurements were performed at the scan rate of 50 mV/s. Electrochemical impedance spectroscopy was carried out at the potential 0 V within the frequency from 100 kHz to 0.1 Hz with the AC amplitude of 10 mV. All electrochemical experiments were performed on AUTOLAB type PGSTAT302N (Metrohm, Switzerland). Electrochemical measurements were carried out without stirring and nitrogen saturation.

## Blood Serum

Blood obtained for laboratory experiments was allowed to coagulate for 24 h without any intervention. Blood serum was obtained after clot removal. The solution was centrifuged for 60 min (800 rev./min) for thorough purification. Blood serum was diluted with the ferro/ferricyanide solution at a ratio of 1:2. Then the solution with the addition of recombinant soluble EGFR was prepared at ratio 1:1:1 (EGFR solution: ferro/ferricyanide solution: blood serum) and ratio 2:1 (EGFR solution: blood serum).

## Results and Discussion

### Optimization of Electrochemical Conditions

The optimization of electrochemical conditions was performed with an emphasis on pH and the presence of the

salts in the solution. The pH could influence the stability of biological molecules and the current response of electrochemical measurements. Moreover, the presence of the salts usually affects the electrochemical measurements, especially in the case of carbon electrodes and  $\text{Cl}^-$  ions in the solution. Chloride ions strongly absorb on the carbon surface, which could decrease the current response of electrodes [38, 39]. Other possible interferences are phosphates, but they absorb activated carbon [40].

Furthermore, these conditions have been studied to verify the use of this sensor under a wide range of conditions. So, commercially purchased screen-printed electrodes modified by streptavidin (SPCEs) were electrochemically tested in two different solutions. The first solution consisted of 0.1 M ferrocyanide and ferricyanide diluted in water and in the second case, the same amount of ferro/ferricyanide was diluted in PBS solution. The electrodes were tested via cyclic voltammetry from the potential  $-1$  V to  $+1$  V at a scan rate of 50 mV/s. Cyclic voltammogram of 0.1 M ferrocyanide and ferricyanide in water solution (Fig. 2A) and cyclic voltammogram of 0.1 M ferrocyanide and ferricyanide in PBS (Fig. 2B) were identical without noticeable changes. So, the presence of the salts in PBS does not interfere with the electrochemical measurement. Then various pH (3, 5, 7, and 9) of both solutions were studied to find an optimal condition and observe changes during the electrochemical measurements. In both cases, the cyclic voltammograms were without the changes (Fig. 2A, B) and the current response was approximately similar. However, the color of solutions was changed from typical yellow to dark green in the case of pH 3.

According to the results, the pH 7 and PBS solution was chosen for further experiments because these conditions are the nearest one to biological samples. And since CV carried on in the water does not differ from the CV realized in the PBS, so the special protocol was not needed. The possible explanation of this is that the streptavidin molecule is stably bound to the electrode surface and the pH value does not influence its electrochemical behavior or molecule conformation.

SPCEs were then modified by the aptamer molecule, where the streptavidin–biotin bond formation was used for anchoring the aptamer to the electrode surface. The aptamer hybrid was bound to the biotinylated DNA oligonucleotide and 3 different solutions were prepared, where the ratio of the aptamer to oligonucleotide was 1:1, 1:5, and 1:10 and the aptamer concentration was 5  $\mu\text{M}$ . It was assumed that at higher concentrations of biotinylated nucleotide, unwanted active sites on the electrode may be blocked, and thus the signal could only be directly associated with soluble EGFR binding. Free active sites (even if they could increase the current response) could serve for oxidation of other biomolecules in the solution and decrease the specificity of electrochemical detection. So, blocking by biotinylated nucleotides is one of options for solving unwanted electrochemical signal from the electroactive sites interacting with other molecules.

When binding the aptamer to the electrode, it was also considered the effect of time on the formation of this bond. The hybridized aptamer solution was diluted 10 $\times$  with a solution and dropped to the electrode (10  $\mu\text{l}$  of solution). The binding of the oligonucleotide-linked aptamer to the

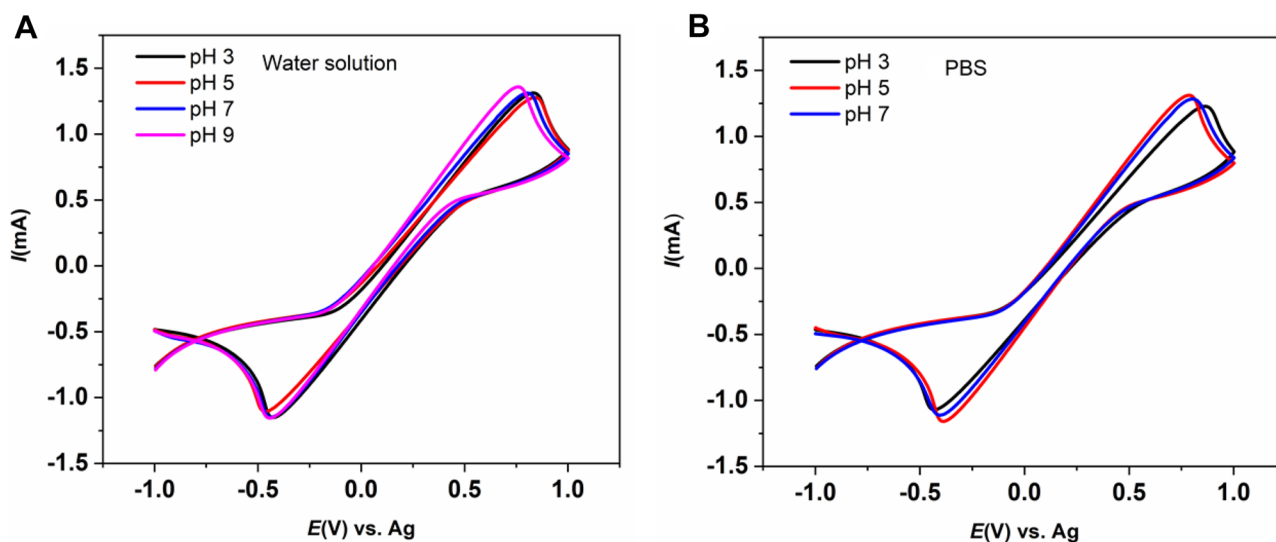


**Fig. 2** **A** Cyclic voltammograms for carbon electrodes modified by streptavidin in the water. **B** Cyclic voltammograms for carbon electrodes modified by streptavidin in PBS solution with 0.1 M ferro/

ferricyanide solution with different pH values. The potential window was within  $-1$  V to 1 V at a scan rate of 50 mV/s

streptavidin took place at 4 °C for 2, 5, 10, 30, and 60 min. A total of 15 samples were obtained, which were rinsed with PBS solution after binding and electrochemically tested. Testing was performed in a solution of 0.1 M ferro/ferricyanide diluted in PBS, which was considered the best in previous measurements. The cyclic voltammetry was used, and the measurement conditions were the same as in the previous case.

Further experiments will be based on the following assumptions. First, it is well known that streptavidin binds very well to the biotin molecule via non-covalent specific interaction. So, aptamer molecules were biotinylated to ensure their anchorage on the streptavidin-modified electrode surface. Another step will be the EGFR binding to the aptamer molecule which is ensured by specificity of aptamer J18. It could be expected that the aptamer and EGFR molecules form the charge-transfer complex which will enhance the charge transfer at phase interface. So, the current response will be influenced by this behavior and increases with concentration of EGFR.

From the cyclic voltammograms (Fig. 3), it can be seen a clear oxidation peak, which is influenced by the binding time of the aptamer to the electrode material. The main goal was to determine the shortest possible time required to prepare the modified electrode. Therefore, we evaluated mainly 3 samples, which were rinsed after 0, 2, and 5 min. The main reason is the fact that the biotin-streptavidin interaction is very rapid [41]. So, it was expected that the bond formation would take a maximum of several minutes. Moreover, it is necessary to find out the shortest possible time for the formation of the bond, so that the preparation of the sensor is efficient and fast.

It could be observed that the current change from the pure electrode was sufficient to conclude that there was a change

**Table 2** Maximum current value for the duration of aptamer binding for different aptamer ratios (1:1, 1:5, and 1:10 ratio of oligonucleotide and aptamer) in 0.1 M ferro/ferricyanide solution, the concentration of aptamer was 0.5  $\mu$ M, pH 7. The maximum current value was found from the cyclic voltammograms

| Time (min) | Maximum current (mA) |       |       |
|------------|----------------------|-------|-------|
|            | 1:1                  | 1:5   | 1:10  |
| 0          | 0.174                | 0.174 | 0.174 |
| 2          | 0.165                | 0.159 | 0.186 |
| 5          | 0.164                | 0.162 | 0.183 |

in the electrode material by binding the aptamer (Table 2). Therefore, it was assumed that a time of 5 min is sufficient for further experiments. At the same time, when comparing solutions with different aptamer: oligonucleotide ratios, it could be seen that the best ratio for our conditions is 1:1, for several reasons. The first reason is the fact that the drop-in current after only 2 min was sufficient (drop-in current was more than 5%) and at the same time not as significant as in the case of the 1:5 ratio (more than 10%). So, the drop-in current was higher than the measurement error but not too significant to ensure enough current response. Another reason is that a decrease in current was expected, if blocking the active sites on the carbon electrode by an aptamer, which is normally a highly conductive material, will reduce its conductivity and thus the current response. Therefore, a 1:1 solution is more suitable for us than a 1:10 solution, and although the current response has increased in the case of a 1:10 ratio, this behavior is not typical and further study would be necessary. But it could be expected that the current increase is only a deviation because values of current response for more than 10 min show plateau and for all the ratios, the value was approx. the same.

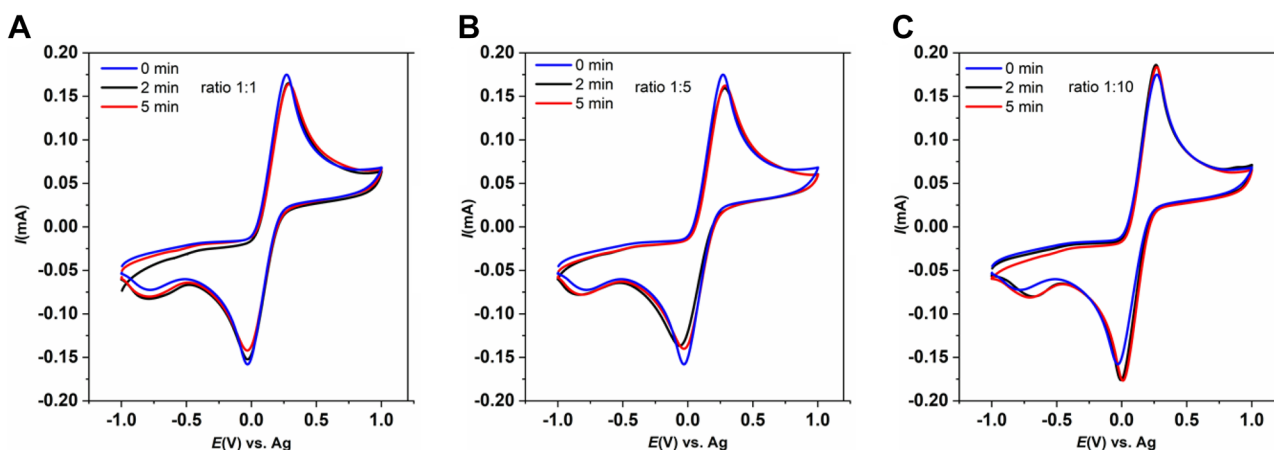


**Fig. 3** Cyclic voltammograms for carbon electrodes modified by streptavidin in the aptamer solution with different concentrations of aptamer (A 1:1, B 1:5, and C 1:10 ratio of oligonucleotide

and aptamer) and with the various duration of aptamer binding in 0.1 M ferro/ferricyanide solution, pH 7. The potential window was within  $-1$  V to  $1$  V at a scan rate of  $50$  mV/s

## Modification of Working Electrode

Despite a series of previously mentioned measurements indicating that the concentration of aptamer is sufficient to alter the signal and record its binding to the electrode, a more concentrated aptamer solution was added to the electrode to ensure that the amount of aptamer would be sufficient to bind the planned soluble EGFR protein concentrations. Another reason for using higher concentration is improvement of electroanalytical characteristics and to achieve a satisfied concentration range.

At first glance, the difference in the current maxima of the cyclic voltammograms can be seen for the dilute solution of the added aptamer and the more concentrated solution (Fig. 4B). After EGFR addition, the current response noticeably decreases. Moreover, as shown in Fig. 4B inset, the control-scrambled aptamer sequence has not bound EGFR.

A much greater effect of aptamer concentration is visible on the EIS spectra (Fig. 4A). Typical for the measured data is fitting by Randles equivalent circuit (Fig. 4A inset). This circuit consists of a solution resistance  $R_1$ , a charge transfer resistance  $R_2$ , a constant phase element  $QPE_1$ , and a specific electrochemical member for diffusion  $Ws_1$ , which is otherwise called a Warburg element. It is clear from the data that not only the transfer of electrons at the phase interface but also the diffusion of electrochemically active particles to the electrode surface will play a role in the electrochemical

process. The electrochemical process is thus also controlled by diffusion, and due to the size of the analyte, i.e., the protein that will be used in further measurements, such behavior was expected. According to changes in the shape of Nyquist diagrams, it can be stated that the addition of the aptamer significantly increased the resistance on the electrical bilayer, which corresponds to the assumption that increasing the amount of aptamer increases the resistance and decreases the current response of the system. The values for individual electrical circuit elements are listed in Table 3. The charge transfer resistance significantly increases from 1734 to 2316  $\Omega$  after the aptamer binding. The charge transfer resistance increase is directly related to the filling up of active sites on the electrode by the aptamer molecule. The charge transfer resistance typically increases during the modification of sandwich-type sensors. The reason is not only the bond creation but also the size of the molecules which block the electrode surface [42–44]. Big molecules such as proteins could block more active sites than are necessary only for bond creation. Moreover, electrode modification by the aptamer with a concentration of 0.5  $\mu\text{M}$  causes the charge transfer resistance to increase to 38,869  $\Omega$ , which represents an increase of more than 16 times. The  $QPE_1$  increased after the EGFR addition from the 39.5 to the 53.6  $\mu\text{F}$ . Moreover, the higher concentration of aptamer ensures more charge-transfer complexes on the electrode surface and causes the double layer capacity to increase to 153  $\Omega$ . Therefore, we

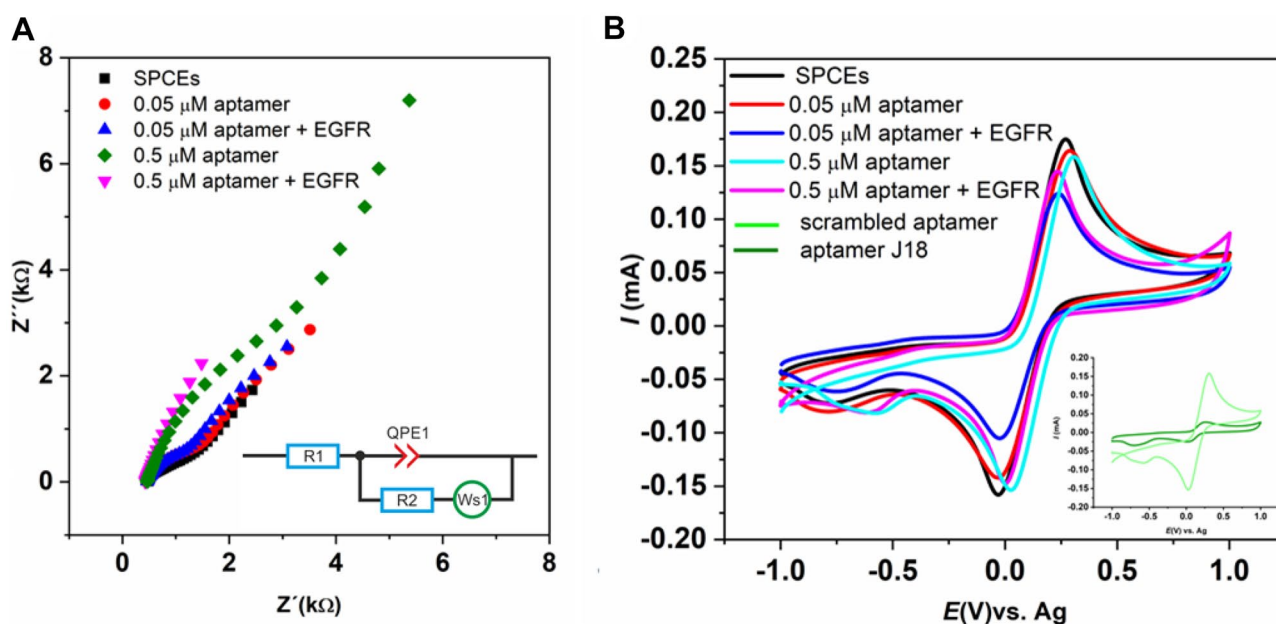


**Fig. 4** **A** Nyquist diagrams for carbon electrodes modified by aptamer and in the presence of 0.5  $\mu\text{M}$  soluble EGFR protein in the solution (at 0 V within the frequency from 100 kHz to 0.1 Hz with the AC amplitude of 10 mV). Inset: The equivalent circuit used for EIS spectra fitting. **B** Cyclic voltammograms under the same conditions. Inset:

Cyclic voltammograms of soluble EGFR for SPCEs modified by the control-scrambled aptamer sequence (green) and aptamer J18 (olive) in 0.1 M ferro/ferricyanide solution, pH 7. The potential window was within  $-1$  V to 1 V at a scan rate of 50 mV/s

**Table 3** The fitting equivalent circuit element parameters for different electrode modifications calculated via Zview software

| Electrode modification                | R1 [ $\Omega$ ]  | QPE1 [ $\mu\text{F}$ ] | R2 [ $\Omega$ ]     | Ws1 (R)         | X2 parameter |
|---------------------------------------|------------------|------------------------|---------------------|-----------------|--------------|
| SPCEs                                 | 468.9 $\pm$ 4.6  | 66.7 $\pm$ 10          | 1734 $\pm$ 17       | 4311 $\pm$ 429  | 0.001        |
| 0.05 $\mu\text{M}$ aptamer J18        | 431.2 $\pm$ 21.5 | 39.5 $\pm$ 3.9         | 2316 $\pm$ 16.2     | 7824 $\pm$ 1173 | 0.002        |
| 0.05 $\mu\text{M}$ aptamer J18 + EGFR | 456.9 $\pm$ 2.9  | 53.6 $\pm$ 4.2         | 2352 $\pm$ 16.4     | 7067 $\pm$ 848  | 0.001        |
| 0.5 $\mu\text{M}$ aptamer J18         | 419.1 $\pm$ 5.8  | 36.4 $\pm$ 1.8         | 13,841 $\pm$ 166    | 7964 $\pm$ 1274 | 0.003        |
| 0.5 $\mu\text{M}$ aptamer J18 + EGFR  | 426.6 $\pm$ 0.8  | 153.2 $\pm$ 3.8        | 38,869 $\pm$ 12,438 | 8034 $\pm$ 1004 | 0.00004      |

used an aptamer solution with a concentration of 0.5  $\mu\text{M}$  in further measurements.

### Electroanalytical Properties of Prepared Aptasensor

To study processes during the electrochemical reaction, the cyclic voltammograms at the different scan rates were measured (Fig. 5). The oxidation peak shift indicates that the electrochemical reaction is an irreversible electrochemical

process. Irreversibility of electrochemical reaction could be influenced by electrode surface modification by aptamer, but it could be influenced by other electrochemical processes for example oligonucleotide oxidation. Based on the dependencies of oxidation peak current on the square root of scan rate ( $R^2=0.99$ ), it could be concluded that the electrochemical reaction is controlled by the diffusion of electroactive species. Also, according to the dependence of oxidation peak current logarithm on scan rate logarithm, where the linear

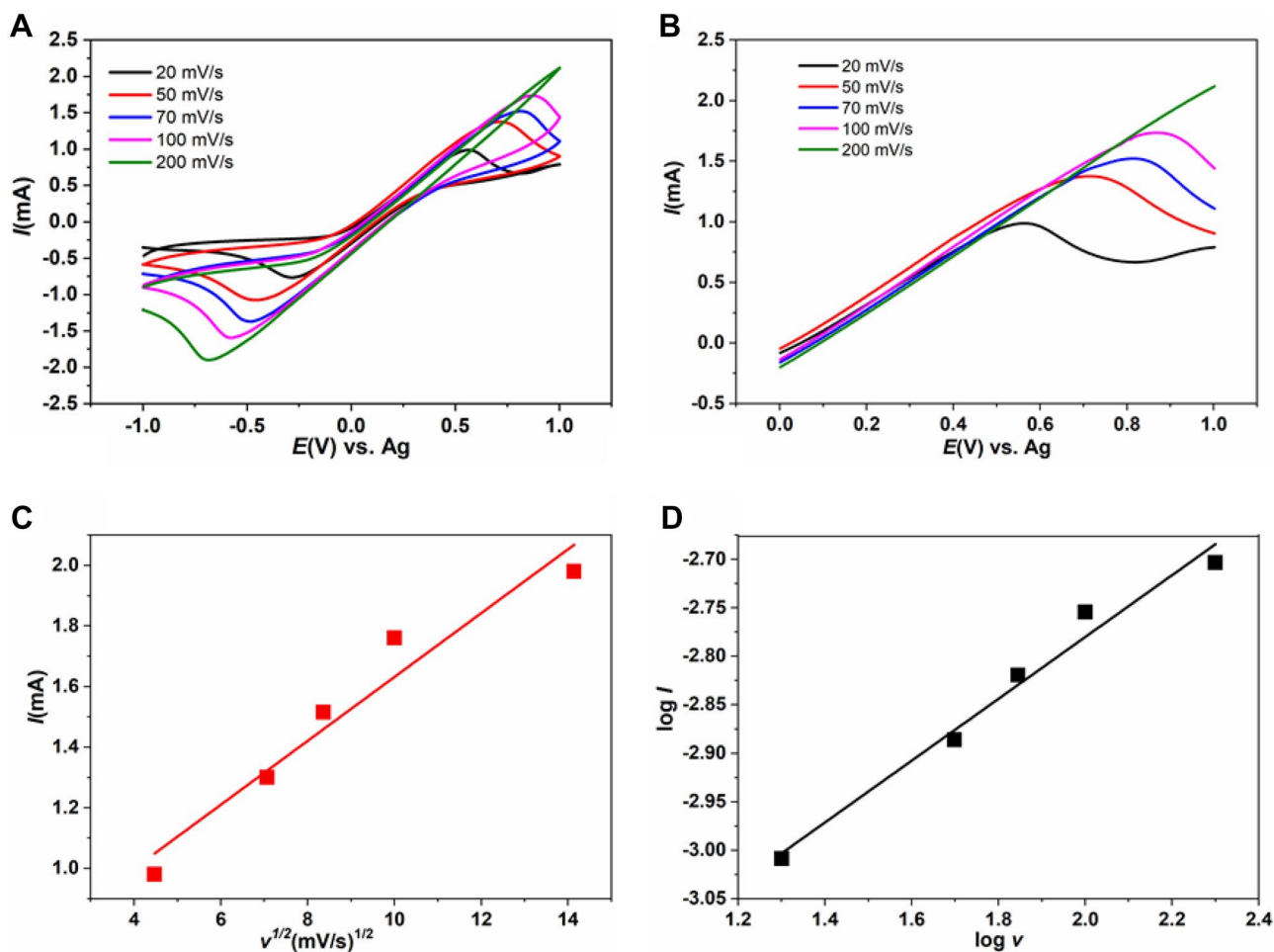


**Fig. 5** A, B Cyclic voltammograms for EGFR solution on SPCEs modified by aptamer at different scan rates (20, 50, 70, 100, and 200 mV/s) in 0.1 M ferro/ferricyanide solution, pH 7. The potential window was within  $-1$  V to  $1$  V at a scan rate of 50 mV/s. C

Dependence of oxidation peak current on the square root of scan rate. D Dependence of oxidation peak current logarithm on scan rate logarithm

regression equation was  $\log I = 0.319 \log v - 3.42$ , it could be concluded that the electrochemical reaction is the diffusion-controlled process. The results correspond with the interpretation of EIS spectra.

Based on the Laviron theory, the number of transferred electrons  $n$  can be determined using the linear regression equation for the linear dependences of peak potential  $E$  on  $\log v$ . Laviron's equation is:

$$E = K + \frac{2.3RT}{(1-\alpha)nF} \log v \quad (1)$$

where  $E$  is the oxidation potential,  $K$  is a constant,  $\alpha$  is the charge transfer coefficient,  $R$  is a gas constant (8.314 J/K/mol),  $T$  is the thermodynamic temperature in K,  $F$  is a Faraday constant (96485 C/mol), and  $v$  is the scan rate. Constant  $K$  represents  $E^0 + \frac{RT}{\alpha n F} \ln \frac{k_s}{k_{-1}}$ , where  $E^0$  is formal potential and  $k_s$  is the standard rate constant of the surface reaction. The linear regression equation was  $E = 0.47 \log v - 0.066$ , where the 0.47 represents value for  $2.3RT/(1-\alpha)nF$  and  $-0.066$  is the value representing constant  $K$ . Calculated number of transferred electrons was 4. It could be supposed that the number of electrons corresponds to the electrochemical reaction of the ferro/ferricyanide system. Moreover, the oligonucleotide chains could be oxidized by using carbon electrodes [45]. So, it could be expected that the oligonucleotide chain is also oxidized during the electrochemical reaction.

To consider the analytical properties of SPCEs, cyclic voltammograms for different concentrations of EGFR from 10 to 500 ng/ml were recorded (Fig. 6). For every

single measurement were used different modified electrodes because the electrode could be used only for one measurement. The solutions for electrochemical measurement were by diluting the 500 ng/ml solution of EGFR. The incubation time was 5 min. The first scan was considered for the measurements. The shifting of the peak could indicate the increasing irreversibility of the electrochemical reaction. So, we expected that the increasing concentration of EGFR influences not only the phase interface but also the reversibility of the electrochemical system. A calibration curve is the dependence of the current peak on the logarithm of the concentration, which exhibits a linear range from 10 to 500 ng/ml. The calculated detection limit was 1.19 ng/ml ( $S/N=3$ ).

Detection properties of the prepared sensor were compared with the properties of other sensors published in the literature (Table 4). The properties of the sensor are competitive with other previously published sensors in the literature.

Also, the EIS spectra were recorded for this concentration range. As could be seen, there are flattened semicircles at the high-frequency region which correspond to the properties of the double layer. The semicircle diameter decreases with the concentration increase. As shown in Fig. 6B, the current response increases with the concentration of EGFR, so according to Ohm's law, the resistance should decrease. It could be expected that the electrochemical process is more complicated than only ferro/ferricyanide electrochemical reaction. So, the formation bond between aptamer EGFR

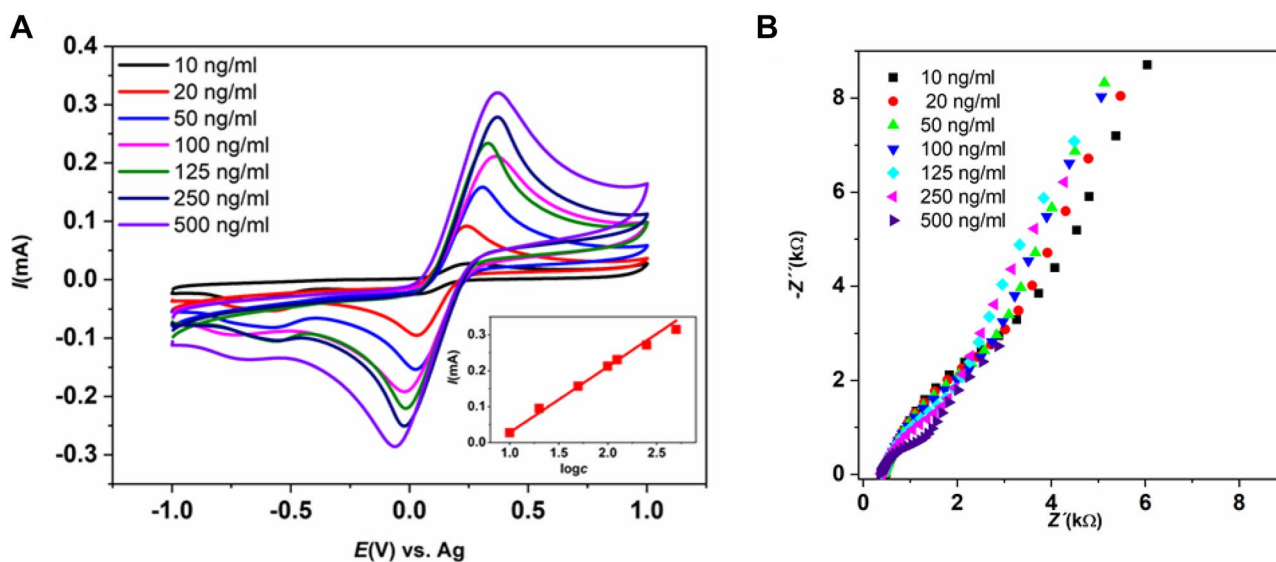


**Fig. 6** **A** Cyclic voltammograms for different concentrations (10, 20, 50, 100, 125, 250, and 500 ng/ml) of EGFR on SPCEs in 0.1 M ferro/ferricyanide solution, pH 7. The potential window was within  $-1$  V to  $1$  V at a scan rate of  $50$  mV/s. Inset: A calibration curve. **B** EIS

spectra for different concentrations of EGFR on SPCEs (at  $0$  V within the frequency from  $100$  kHz to  $0.1$  Hz with the AC amplitude of  $10$  mV)



**Table 4** List of recently published EGFR and cancer-relevant biomarkers electrochemical sensors

| Electrode material                                       | Target | Linear range          | Limit of detection | Sensitivity | Ref       |
|--|--------|-----------------------|--------------------|-------------|-----------|
| Hyper-branched gold nanostructure (ns@gold) immunosensor | EGFR   | 10 pg/ml–100 ng/ml    | 6.9 pg/ml          | -           | [13]      |
| Anti-EGFRab/DTSP/Au immunoelectrode leads                | EGFR   | 1 pg/ml–100 ng/ml     | 1 pg/ml            | 0.002 mA/mM | [5]       |
| Multiple signal biosensors                               | EGFR   | 0–107 ng/ml           | 94.7 pg/ml         | -           | [6]       |
| Silica-chitosan nanoplatfrom immunosensor                | EGFR   | 0–50 ng/ml            | 1.37 pg/ml         | -           | [14]      |
| Ni-OTC/rGO/f-OMC/PGE                                     | EGFR   | 9.47–284.1 $\mu$ g/ml | 11.3 pg/ml         | 18.8 mA/mM  | [1]       |
| Peptide-based biosensor                                  | EGFR   | 1000–100 ng/ml        | 0.037 pg/ml        | -           | [11]      |
| rGO-Chit aptasensor                                      | HER2   | 2–75 ng/ml            | 0.21 ng/ml         | -           | [46]      |
| rGO aptasensor   | CEA    | 0.1 fg/ml–5 pg/ml     | 0.1 fg/ml          | -           | [47]      |
| rGO/GCE aptasensor                                       | CEA    | 80 ag/ml–950 fg/ml    | 80 ag/ml           | -           | [48]      |
| SPCEs aptasensors  | EGFR   | 10–500 ng/ml          | 1190 pg/ml         | 1.82 mA/mM  | This work |

CEA Carcinoembryonic Antigen, *Chit* Chitosan, *DTSP* Dithiobissuccimidyl Propionate, *f-OMC* Carbonyl Functionalized Ordered Mesoporous Carbon, *GCE* Glassy Carbon Electrode, *Ni-OTC FNPs-Ni(II)* Oxytetracycline Metallopolymer Nanoparticles, *PGE* Pencil Graphite Electrode, *rGO* Reduce Graphene Oxide

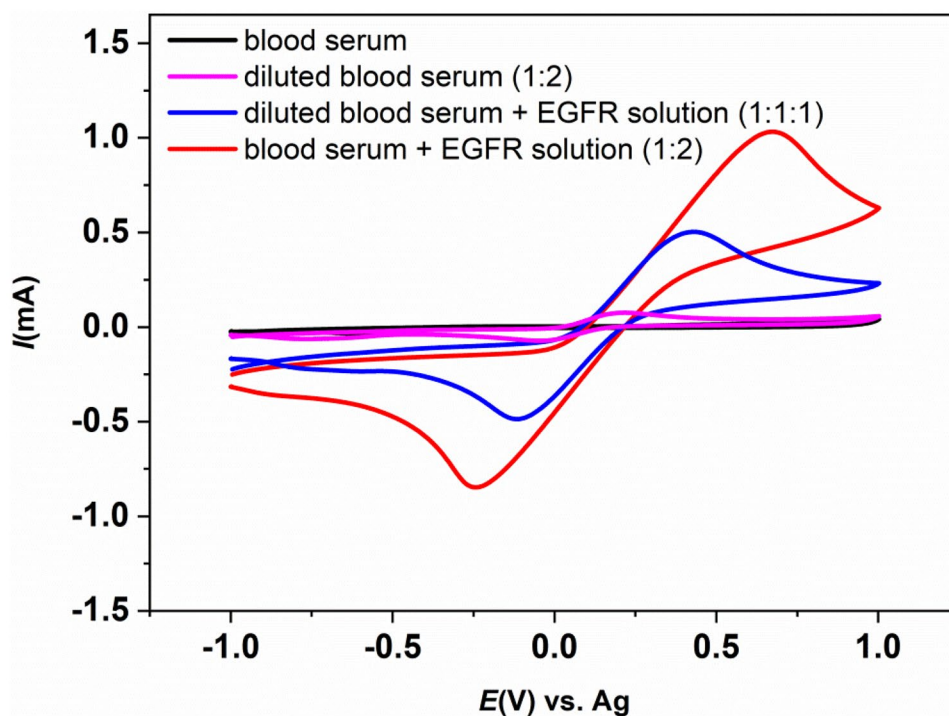
could increase the conductivity of the phase interface, because of the formation of charge-transfer complexes.

Based on this, it could be assumed that this type of modified electrodes can be used not only in amperometric but also in an impedimetric type of sensor.

Blood serum was used to verify the method used for real samples analysis. Blood serum was diluted in different ratios with a solution of ferro/ferricyanide and EGFR diluted in this solution. Three solutions were prepared with the same concentration of salt and blood serum components, but with an increasing concentration of EGFR, as shown

in Fig. 7. Blood serum was mixed with 0.1 M ferro/ferricyanide solution in ratio 1:2 (pink curve), and blood serum was also mixed with 0.1 M ferro/ferricyanide solution and EGFR–0.1 M ferro/ferricyanide solution (500 ng/ml concentration of EGFR) in ratio 1:1:1 (blue curve). So, the concentration of EGFR in the final solution was approx. 167 ng/ml, and blood serum mixed with EGFR–0.1 M ferro/ferricyanide solution (500 ng/ml concentration of EGFR) in ratio 1:2 (red curve). The concentration of EGFR was approx. 333 ng/ml in the last-mentioned solution. The measurements were performed under the same condition as

**Fig. 7** Cyclic voltammograms for blood serum solutions: blood serum mixed with 0.1 M ferro/ferricyanide solution in ratio 1:2 (pink curve), blood serum mixed with 0.1 M ferro/ferricyanide solution, and EGFR–0.1 M ferro/ferricyanide solution (500 ng/ml concentration of EGFR) in ratio 1:1:1 (blue curve), and blood serum mixed with EGFR–0.1 M ferro/ferricyanide solution (500 ng/ml concentration of EGFR) in ratio 1:2 (red curve). The potential window was within –1 V to 1 V at a scan rate of 50 mV/s



the calibration curve, without any regeneration steps. The current response increases with the increasing concentration of EGFR. Moreover, the blood serum solution contains all the biological molecules which could be active within the used potential window, so the selectivity of the electrode could be considered as satisfied. According to the results, prepared electrodes are promising candidates to detect soluble EGFR in real samples.

The reproducibility of the electrode was calculated for the modified electrodes. The reproducibility was more than 97.5%. The screen-printed electrodes are for single use only by the manufacturer, so the repeatability of the measurement on the single electrode is not possible. On the other hand, the practical use of the screen-printed electrodes could be demonstrated on the glucose sensor example; moreover, the streptavidin-modified electrodes are already commercially produced. So, the modified electrodes display a predisposition to commercial use.

## Conclusions

Here we report a simple electrochemical aptasensor for soluble EGFR detection, without the addition of any noble metals. Aptamers were the selective platform for the specific detection of soluble EGFR. The conditions for electrochemical sensing were optimized and pH 7 and PBS solution was chosen as the best option for further measurements. Also, the time of aptamer binding to the electrode surface was optimized. In addition, the mechanism of electrochemical reaction was studied. It was assumed that the electrochemical reaction is the diffusion-controlled process, and it was supported by the EIS results. SPCEs sensor displays a wide linear range from 10 to 500 ng/ml and a low detection limit of 1.19 ng/ml. Moreover, the SPCEs sensor can be used not only as an amperometric but also as an impedimetric sensor. EGFR detection was successfully tested also in b, so the prepared sensor could be a very promising one for the real samples detection.

**Author Contribution** I. Š. and J. S. conceived of the presented idea. J. S. developed the theory and wrote the manuscript with support from I. Š. and M. P. I. Š. carried out the electrochemical experiments and M. P. and D. B. carried out the aptamer development. P. J. and R. O. supervised the work with the purchased blood serum realized under specific conditions. Both R. O. and P. J. authors contributed to the final version of the manuscript.

**Funding** This research was funded by Slovak Research and Development Agency, grant number APVV-PP-COVID-20-0036.

## Declarations

**Conflict of Interest** The authors declare no competing interests.

## References

1. Y. Shoja, A. Kermanpur, F. Karimzadeh, *Biosens. Bioelectron.* **113**, 108 (2018)
2. Y. Yang, X. Yang, Y. Yang, Q. Yuan, *Carbon N. Y.* **129**, 380 (2018)
3. R. Elshafey, A.C. Tavares, M. Siaj, M. Zourob, *Biosens. Bioelectron.* **50**, 143 (2013)
4. H. Ilkhani, M. Sarparast, A. Noori, S.Z. Bathaie, M.F. Mousavi, *Biosens. Bioelectron.* **74**, 491 (2015)
5. A. Vasudev, A. Kaushik, S. Bhansali, *Biosens. Bioelectron.* **39**, 300 (2013)
6. X.H. Weng, X.W. Xu, P.F. Huang, Z.J. Liu, A.L. Liu, Z.Y. Lin, W. Chen, X.H. Lin, *J. Electroanal. Chem.* **853**, 113555 (2019)
7. X.W. Xu, X.H. Weng, C.L. Wang, W.W. Lin, A.L. Liu, W. Chen, X.H. Lin, *Biosens. Bioelectron.* **80**, 411 (2016)
8. V. Müller, I. Witzel, K. Pantel, S. Krenkel, H.J. Lück, R. Neumann, T. Keller, J. Dittmer, F. Jänicke, C. Thomssen, *Anticancer Res.* **26**, 1479 (2006)
9. K.A. Adamczyk, S. Klein-Scory, M.M. Tehrani, U. Warnken, W. Schmiegel, M. Schnölzer, I. Schwarte-Waldhoff, *Life Sci.* **89**, 304 (2011)
10. I. Kappers, M. A. Vollebergh, H. Van Tinteren, C. M. Korse, L. L. Nieuwenhuis, J. M. G. Bonfrer, H. M. Klomp, N. Van Zandwijk, M. M. Van Den Heuvel, *Ecancermedalscience* **4**, (2010)
11. R. Li, H. Huang, L. Huang, Z. Lin, L. Guo, B. Qiu, G. Chen, *Electrochim. Acta* **109**, 233 (2013)
12. Y. Wang, W. Gao, M. Wu, X. Zhang, W. Liu, Y. Zhou, C. Jia, H. Cong, X. Chen, J. Zhao, *Talanta* **225**, 122057 (2021)
13. S. Bakshi, S. Mehta, T. Kumeria, M. J. A. Shiddiky, A. Popat, S. Choudhury, S. Bose, R. Nayak, *Sensors Actuators. B Chem.* **326**(2021)
14. F. G. Ortega, S. V. Piguillem, G. A. Messina, G. R. Tortella, O. Rubilar, M. I. J Castillo, J. A. Lorente, M. J. Serrano, J. Raba, M. A. Fernández Baldo, *Talanta* **194**, 243 (2019)
15. T. Guo, W. Li, L. Qian, X. Yan, D. Cui, J. Zhao, H. Ni, X. Zhao, Z. Zhang, X. Li, L. Huang, L. Wang, *J. Pharm. Biomed. Anal.* **190**, 113522 (2020)
16. J.C. Chen, S. Sadhasivam, F.H. Lin, *Process Biochem.* **46**, 543 (2011)
17. X.H. Weng, X.W. Xu, C.L. Wang, W.W. Lin, A.L. Liu, W. Chen, X.H. Lin, *J. Pharm. Biomed. Anal.* **150**, 176 (2018)
18. A. Khanmohammadi, A. Aghaie, E. Vahedi, A. Qazvini, M. Ghanei, A. Afkhami, A. Hajian, H. Bagheri, *Talanta* **206**, 120251 (2020)
19. C. Yang, M.E. Denno, P. Pyakurel, B.J. Venton, *Anal. Chim. Acta* **887**, 17 (2015)
20. W. Zhang, S. Zhu, R. Luque, S. Han, L. Hu, G. Xu, *Chem. Soc. Rev.* **45**, 715 (2016)
21. P. Bollella, G. Fusco, C. Tortolini, G. Sanz??, G. Favero, L. Gorton, R. Antiochia, *Biosens. Bioelectron.* **89**, 152 (2017)
22. R.A.S. Couto, J.L.F.C. Lima, M.B. Quinaz, *Talanta* **146**, 801 (2016)
23. O.D. Renedo, M.A. Alonso-Lomillo, M.J.A. Martínez, *Talanta* **73**, 202 (2007)
24. M. Li, D.W. Li, G. Xiu, Y.T. Long, *Curr. Opin. Electrochem.* **3**, 137 (2017)
25. M. Trojanowicz, *TrAC - Trends Anal. Chem.* **84**, 22 (2016)
26. H.M. Mohamed, *TrAC - Trends Anal. Chem.* **82**, 1 (2016)
27. F. Arduini, L. Micheli, D. Moscone, G. Palleschi, S. Piermarini, F. Ricci, G. Volpe, *TrAC - Trends Anal. Chem.* **79**, 114 (2016)
28. M. Li, Y.T. Li, D.W. Li, Y.T. Long, *Anal. Chim. Acta* **734**, 31 (2012)
29. S. Zhang, F. Rong, C. Guo, F. Duan, L. He, M. Wang, Z. Zhang, M. Kang, M. Du, *Coord. Chem. Rev.* **439**, 213948 (2021)

30. Oszos Mehmet, Electrochemical DNA biosensors (Pan Stanford Publishing, 2012)
31. K. Han, Z. Liang, N. Zhou, *Sensors* **10**, 4541 (2010)
32. C. Tuerk, L. Gold, *Science* **249**, 505 (1990)
33. A.D. Ellington, J.W. Szostak, *Nature* **346**, 818 (1990)
34. K.A. Afonin, M. Viard, A.Y. Koyfman, A.N. Martins, W.K. Kasprzak, M. Panigaj, R. Desai, A. Santhanam, W.W. Grabow, L. Jaeger, E. Heldman, J. Reiser, W. Chiu, E.O. Freed, B.A. Shapiro, *Nano Lett.* **14**, 5662 (2014)
35. M. Panigaj, M. B. Johnson, W. Ke, J. McMillan, E. A. Goncharova, M. Chandler, and K. A. Afonin, *ACS Nano* (2019)
36. N. Li, T. Larson, H.H. Nguyen, K.V. Sokolov, A.D. Ellington, *Chem. Commun.* **46**, 392 (2010)
37. N. Li, J. Ebright, G. Stovall, X. Chen, A. Singh, H. Syrett, A.D. Ellington, A. Syrett, A.D. Ellington, *J. Proteome Res.* **8**, 2438 (2009)
38. P. Boonruam, P. Wattanachai, S. Upasen, *Proceedings 2*, 1314 (2018)
39. Z. Sun, L. Chai, Y. Shu, Q. Li, M. Liu, D. Qiu, *Colloids Surfaces A Physicochem. Eng. Asp.* **530**, 53 (2017)
40. A.K. Ouakouak, L. Youcef, *Sens. Lett.* **14**, 600 (2016)
41. H. Yang, Q. Zhang, X. Liu Data analysis, Y. Yang Data analysis, Y. Yang, M. Liu, P. Li, and Y. Zhou, *Food Chem.* 316, 126356 (2020)
42. J. Fan, W. Yang, *Sensors actuators B Chem.* **353**, 131100 (2022)
43. T.T.Q. Nguyen, E.R. Kim, M.B. Gu, *Biosens. Bioelectron.* **198**, 113835 (2022)
44. M. Naseri, A. Halder, M. Mohammadniaei, M. Prado, J. Ashley, Y. Sun, *Electrochim. Acta* **389**, 138644 (2021)
45. A.F. Tikum, J.W. Ko, S. Kim, J. Kim, *ACS Omega* **3**, 15464 (2018)
46. A. Tabasi, A. Noorbakhsh, E. Sharifi, *Biosens. Bioelectron.* **95**, 117 (2017)
47. W. Wang, L. Ge, X. Sun, T. Hou, F. Li, *A.C.S. Appl. Mater. Interfaces* **7**, 28566 (2015)
48. L. Ge, W. Wang, X. Sun, T. Hou, F. Li, *Anal. Chem.* **88**, 2212 (2016)

**Publisher's Note** Springer Nature remains neutral with regard to jurisdictional claims in published maps and institutional affiliations.